Research Article | Vol. 9, No. 1 | 1 Jan 2018 | BIOMEDICAL OPTICS EXPRESS 131
Biomedical Optics EXPRESS

# Concurrent measurement of skeletal muscle blood flow during exercise with diffuse correlation spectroscopy and Doppler ultrasound

CHANDAN-GANESH BANGALORE-YOGANANDA,[1,3] RYAN ROSENBERRY,[2,3] SAGAR SONI,[1] HANLI LIU,[1] MICHAEL D. NELSON,[1,2] AND FENGHUA TIAN[1,*]

[1]*Department of Bioengineering, The University of Texas at Arlington, 500 UTA Blvd., Arlington, TX 76010, USA*
[2]*Department of Kinesiology, The University of Texas at Arlington, 411 S. Nedderman Dr., Arlington, TX 76010, USA*
[3]*Two authors contributed equally*
[*]*fenghua.tian@uta.edu*

**Abstract:** Noninvasive, direct measurement of local muscle blood flow in humans remains limited. Diffuse correlation spectroscopy (DCS) is an emerging technique to measure regional blood flow at the microvascular level. In order to better understand the strengths and limitations of this novel technique, we performed a validation study by comparing muscle blood flow changes measured with DCS and Doppler ultrasound during exercise. Nine subjects were measured (all males, 27.4 ± 2.9 years of age) for a rhythmic handgrip exercise at 20% and 50% of individual maximum voluntary contraction (MVC), followed by a post-exercise recovery. The results from DCS and Doppler ultrasound were highly correlated ($R$ = 0.99 ± 0.02). DCS was more reliable and less susceptible to motion artifact.



**OCIS codes:** (000.1430) Biology and medicine; (120.4640) Optical instruments; (170.1610) Clinical applications; (170.3890) Medical optics instrumentation; (170.6280) Spectroscopy, fluorescence and luminescence.

## References and links

1. American College of Sports Medicine, W. J. Chodzko-Zajko, D. N. Proctor, M. A. F. Singh, C. T. Minson, C. R. Nigg, G. J. Salem, and J. S. Skinner, "Exercise and physical activity for older adults," Med. Sci. Sports Exerc. **41**(7), 1510–1530 (2009).
2. S. T. Aspenes, T. I. Nilsen, E. A. Skaug, G. F. Bertheussen, Ø. Ellingsen, L. Vatten, and U. Wisløff, "Peak oxygen uptake and cardiovascular risk factors in 4631 healthy women and men," Med. Sci. Sports Exerc. **43**(8), 1465–1473 (2011).
3. S. N. Blair, H. W. Kohl 3rd, C. E. Barlow, R. S. Paffenbarger, Jr., L. W. Gibbons, and C. A. Macera, "Changes in physical fitness and all-cause mortality. A prospective study of healthy and unhealthy men," JAMA **273**(14), 1093–1098 (1995).
4. S. N. Blair, H. W. Kohl 3rd, R. S. Paffenbarger, Jr., D. G. Clark, K. H. Cooper, and L. W. Gibbons, "Physical fitness and all-cause mortality. A prospective study of healthy men and women," JAMA **262**(17), 2395–2401 (1989).
5. D. H. Paterson, D. Govindasamy, M. Vidmar, D. A. Cunningham, and J. J. Koval, "Longitudinal study of determinants of dependence in an elderly population," J. Am. Geriatr. Soc. **52**(10), 1632–1638 (2004).
6. M. Venturelli, F. Schena, and R. S. Richardson, "The role of exercise capacity in the health and longevity of centenarians," Maturitas **73**(2), 115–120 (2012).
7. R. Bi, J. Dong, C. L. Poh, and K. Lee, "Optical methods for blood perfusion measurement-theoretical comparison among four different modalities," J. Opt. Soc. Am. A **32**(5), 860–866 (2015).
8. Y. Shang, L. Chen, M. Toborek, and G. Yu, "Diffuse optical monitoring of repeated cerebral ischemia in mice," Opt. Express **19**(21), 20301–20315 (2011).
9. M. N. Kim, B. L. Edlow, T. Durduran, S. Frangos, R. C. Mesquita, J. M. Levine, J. H. Greenberg, A. G. Yodh, and J. A. Detre, "Continuous optical monitoring of cerebral hemodynamics during head-of-bed manipulation in brain-injured adults," Neurocrit. Care **20**(3), 443–453 (2014).
10. C. Zhou, S. A. Eucker, T. Durduran, G. Yu, J. Ralston, S. H. Friess, R. N. Ichord, S. S. Margulies, and A. G. Yodh, "Diffuse optical monitoring of hemodynamic changes in piglet brain with closed head injury," J. Biomed. Opt. **14**(3), 034015 (2009).

#306844 https://doi.org/10.1364/BOE.9.000131
Journal © 2018 Received 12 Sep 2017; revised 26 Nov 2017; accepted 5 Dec 2017; published 8 Dec 2017

Biomedical Optics EXPRESS


11. G. Yu, T. F. Floyd, T. Durduran, C. Zhou, J. Wang, J. A. Detre, and A. G. Yodh, "Validation of diffuse correlation spectroscopy for muscle blood flow with concurrent arterial spin labeled perfusion MRI," Opt. Express **15**(3), 1064–1075 (2007).
12. D. P. Casey, T. B. Curry, and M. J. Joyner, "Measuring muscle blood flow: a key link between systemic and regional metabolism," Curr. Opin. Clin. Nutr. Metab. Care **11**(5), 580–586 (2008).
13. J. Dong, R. Bi, J. H. Ho, P. S. Thong, K. C. Soo, and K. Lee, "Diffuse correlation spectroscopy with a fast Fourier transform-based software autocorrelator," J. Biomed. Opt. **17**(9), 097004 (2012).
14. M. D. Herr, C. S. Hogeman, D. W. Koch, A. Krishnan, A. Momen, and U. A. Leuenberger, "A real-time device for converting Doppler ultrasound audio signals into fluid flow velocity," Am. J. Physiol. Heart Circ. Physiol. **298**(5), H1626–H1632 (2010).
15. A. Keys, F. Fidanza, M. J. Karvonen, N. Kimura, and H. L. Taylor, "Indices of relative weight and obesity," J. Chronic Dis. **25**(6), 329–343 (1972).
16. K. Gurley, Y. Shang, and G. Yu, "Noninvasive optical quantification of absolute blood flow, blood oxygenation, and oxygen consumption rate in exercising skeletal muscle," J. Biomed. Opt. **17**(7), 075010 (2012).
17. T. Durduran, R. Choe, W. B. Baker, and A. G. Yodh, "Diffuse optics for tissue monitoring and tomography," Rep. Prog. Phys. **73**(7), 076701 (2010).
18. S. Prahl, *"Optical Absorption of Hemoglobin,"* http://omlc.org/spectra/hemoglobin/.
19. D. H. Thijssen, T. H. Schreuder, S. W. Newcomer, M. H. Laughlin, M. T. Hopman, and D. J. Green, "Impact of 2-weeks continuous increase in retrograde shear stress on brachial artery vasomotor function in young and older men," J. Am. Heart Assoc. **4**(10), e001968 (2015).
20. E. Iwamoto, K. Katayama, and K. Ishida, "Exercise intensity modulates brachial artery retrograde blood flow and shear rate during leg cycling in hypoxia," Physiol. Rep. **3**(6), e12423 (2015).
21. T. H. Schreuder, D. J. Green, M. T. Hopman, and D. H. Thijssen, "Acute impact of retrograde shear rate on brachial and superficial femoral artery flow-mediated dilation in humans," Physiol. Rep. **2**(1), e00193 (2014).
22. T. E. Ryan, W. M. Southern, M. A. Reynolds, and K. K. McCully, "A cross-validation of near-infrared spectroscopy measurements of skeletal muscle oxidative capacity with phosphorus magnetic resonance spectroscopy," J. Appl. Physiol. **115**(12), 1757–1766 (2013).
23. G. Yu, T. Durduran, G. Lech, C. Zhou, B. Chance, E. R. Mohler 3rd, and A. G. Yodh, "Time-dependent blood flow and oxygenation in human skeletal muscles measured with noninvasive near-infrared diffuse optical spectroscopies," J. Biomed. Opt. **10**(2), 024027 (2005).
24. B. Henry, M. Zhao, Y. Shang, T. Uhl, D. T. Thomas, E. S. Xenos, S. P. Saha, and G. Yu, "Hybrid diffuse optical techniques for continuous hemodynamic measurement in gastrocnemius during plantar flexion exercise," J. Biomed. Opt. **20**(12), 125006 (2015).
25. Y. Shang, K. Gurley, B. Symons, D. Long, R. Srikuea, L. J. Crofford, C. A. Peterson, and G. Yu, "Noninvasive optical characterization of muscle blood flow, oxygenation, and metabolism in women with fibromyalgia," Arthritis Res. Ther. **14**(6), R236 (2012).
26. N. Munk, B. Symons, Y. Shang, R. Cheng, and G. Yu, "Noninvasively measuring the hemodynamic effects of massage on skeletal muscle: A novel hybrid near-infrared diffuse optical instrument," J. Bodyw. Mov. Ther. **16**(1), 22–28 (2012).
27. D. A. Boas, S. Sakadžić, J. Selb, P. Farzam, M. A. Franceschini, and S. A. Carp, "Establishing the diffuse correlation spectroscopy signal relationship with blood flow," Neurophotonics **3**(3), 031412 (2016).


## 1. Introduction

Skeletal muscle blood flow is a key determinant of aerobic capacity, which is an independent predictor of quality of life and cardiovascular disease morbidity and mortality [1–6]. Monitoring skeletal muscle blood flow regulation is therefore essential to provide pathophysiological insight and clinical diagnosis, as well as to evaluate treatment efficacy. Numerous noninvasive methods exist to quantify skeletal muscle blood flow, such as venous occlusion plethysmography. However, these techniques measure changes in bulk conduit flow and do not provide regional (microvascular) or temporal information. In contrast, arterial-spin-labeled magnetic resonance imaging (ASL-MRI) and positron emission tomography (PET) can measure skeletal muscle microvascular perfusion, but are expensive and technically challenging and therefore not available to all clinics or laboratories. Exposure to radiation, as with PET, also limits application to certain populations.

Near-infrared diffuse correlation spectroscopy (DCS) is an emerging technique for measurement of regional blood flow at the microvascular level. In addition to being completely noninvasive and portable, DCS has a relatively high temporal resolution and a relatively large penetration depth [7]. Moreover, DCS has been validated in a variety of organs and tissues, against several different standards, including laser Doppler [8], Xenon-CT [9], fluorescent microsphere flow measurements [10], and ASL-MRI [11]. Unfortunately, the

Biomedical Optics EXPRESS

vast majority of these validation experiments were performed on the brain, which is inherently less susceptible to motion artifact (especially during exercise). In fact, the only prior investigation to validate DCS in skeletal muscle was done using a cuff inflation and deflation protocol in which the muscle remains virtually motionless [11].

The purpose of the present study was therefore to validate DCS-derived skeletal muscle blood flow measurements against Doppler ultrasound during rhythmic exercise. Doppler ultrasound is currently the most commonly used flow imaging modality to assess skeletal muscle blood flow regulation and kinetics during exercise [12]. Its high temporal resolution provides a perfect opportunity for flow synchronization between the two modalities, providing comprehensive and comparative evaluation of muscle blood flow kinetics to improve our understanding of DCS.

## 2. Materials and methods

### *2.1 Subjects*

Healthy subjects between 20–35 years of age were recruited from the local community of the University of Texas at Arlington (UTA). The experimental protocol was approved by the UTA Institutional Review Board (IRB). Written informed consent was obtained from each subject prior to the experiment.

### *2.2 Instruments*

A single-wavelength DCS system was used to measure the relative changes in muscle blood flow. The system was built in-house and validated through phantom and human arm cuff occlusion experiments. It consists of a continuous-wave, long-coherence-length laser diode (785 nm & 100 mW, Crystalaser Inc., Reno, NV) as light source and a single-photon-counting avalanche photodiode (APD) as detector (SPCM-AQRH-14-FC, Pacer USA LLC., Palm Beach Gardens, FL). The output of the APD is connected to a computer with a 32-bit, 8-channel data acquisition card (PCI-6602, National Instruments Corp., Austin, TX). A LabVIEW (National Instruments Corp., Austin, TX) program was developed for photon counting. Similar to Dong et al. [13], a software autocorrelator calculates the autocorrelation function and absolute intensity (sum of photon counts) of diffused light, which reduced overall cost and complexity of the system as compared with a hardware autocorrelator. A 3D-printed probe was used to hold a multi-mode fiber (125 μm in core diameter) from the source laser and a single-mode fiber (5 μm in core diameter) to the APD detector. The probe was affixed directly to the left forearm (the exercising side) over the belly of the flexor digitorum profundus, the primary muscle used during handgrip exercise (Fig. 1), using black Velcro strips. The source-to-detector distance was 1.5 cm. The data sampling rate was 1 Hz.

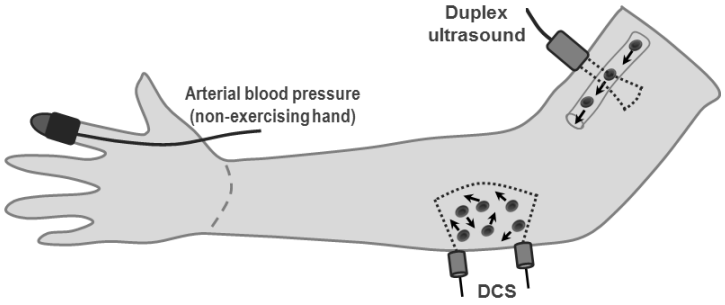


Fig. 1. Schematic of experimental setup. Blood pressure was measured using a servo-controlled finger photoplethysmography on the middle or index finger of the right hand (the non-exercising side). Brachial artery blood flow velocity and diameter were measured on the right upper arm with a duplex ultrasound system. The DCS probe was affixed to the left forearm over the belly of the flexor digitorum profundus.

Biomedical Optics EXPRESS

Brachial artery blood flow velocity and diameter were measured with a duplex ultrasound system (Vivid-i, GE Healthcare, Little Chalfont, United Kingdom) on the left upper arm (the exercising side). This system had a 12-MHz linear array probe with 60 degree of insonation. The ultrasound gate was optimized to ensure complete insonation of the entire vessel cross-section with constant intensity. The continuous Doppler audio signal was converted to real-time blood flow velocity waveforms using a validated Doppler audio converter [14] and recorded using a PowerLab data acquisition system (ADInstruments Inc., Boulder, CO). Brachial artery diameter was measured with B-mode ultrasound imaging, which was conducted once in each of the four experimental stages (to be described in section *2.3*).

Noninvasive arterial blood pressure was measured using a servo-controlled finger photoplethysmography (Human NIBP Controller, ADInstruments Inc., Boulder, CO) that was placed on the middle or index finger of the right hand (the non-exercising side) and supported on a bedside table positioned at heart level. In addition, an automated sphygmomanometer (Welch Allyn, Skaneateles Fall, NY) recorded resting blood pressure periodically, and was used to verify and calibrate the finger photoplethysmography measurements.

The analog outputs from Doppler ultrasound and arterial blood pressure module, along with the amplified signal from a Smedley handgrip dynamometer (Stoelting Co., Wood Dale, IL), were connected to a high-performance, physiological data acquisition system (PowerLab 16/35, ADInstruments Inc., Boulder, CO) for simultaneous data recording. Since the DCS system does not have an analog output, a TTL gating signal to the PowerLab was used to time align the DCS data (to be described in section *2.4.2*) with all the other physiological signals.

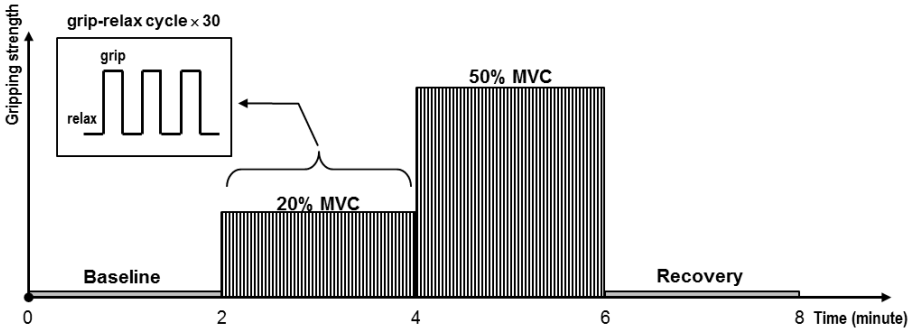


Fig. 2. Paradigm of the handgrip exercise experiment. The experiment consisted of four stages: baseline, rhythmic handgrip exercise at 20% and then 50% of maximal voluntary contraction (MVC), and post-exercise recovery. Each stage lasted two minutes. During the exercise period, the subject repeatedly griped the dynamometer for two seconds and then released for two seconds.

### *2.3 Experimental protocols*

All experiments were performed in a dimly-lit, temperature controlled room. Upon arrival to the laboratory, body weight and height were measured using a standard stadiometer and weight scale, and body mass index (BMI) [15] was derived. Subjects were then positioned supine on a bed and instrumented for finger photoplethysmography, ultrasound, and DCS. The handgrip dynamometer was positioned on the subject's left side, so that the arm could comfortably be extended and supported at heart level. Prior to any data collection, subjects were instructed to grip the handgrip dynamometer as hard as possible to establish individual maximal voluntary contraction (MVC). Subjects were then given a short break prior to data collection. After hemodynamic data stabilized, baseline data were recorded, followed by rhythmic handgrip exercise at 20% and then 50% of individual MVC respectively, and post-exercise recovery. Each stage lasted two minutes (Fig. 2). During the exercise period, the subject repeatedly griped the dynamometer for two seconds and then relaxed for two seconds, guided by a recorded voice prompt. To minimize muscle-fiber motion artifact during exercise,

Biomedical Optics EXPRESS

data were recorded only during the relaxation phase of the handgrip duty cycle (i.e., two DCS data points per cycle, which were then averaged to derive a single reading per cycle.), using the previously described gating algorithm [16].

### *2.4 Data analysis*

#### 2.4.1 Finger blood pressure and Doppler ultrasound

Arterial blood pressure and Doppler ultrasound data were analyzed offline by a single observer (RR) using the LabChart Pro software environment (ADInstruments Inc., Boulder, CO). For the real-time arterial blood pressure waveforms, a peak-detection algorithm was applied to identify the systolic and diastolic components as the peak and valley of each arterial pulse. Then mean arterial pressure (MAP, mmHg) was calculated on a beat-to-beat basis.

Similarly, mean blood flow velocity (MBFV, cm/s) was calculated as the beat-to-beat average from the real-time Doppler ultrasound waveforms. Then brachial artery blood flow (ml/min) was estimated as MBFV × $\pi r^2$ × 60, where r is the radius of brachial artery (cm) measured with B-mode ultrasound imaging. It is noted that the radius of brachial artery was measure once in each experimental stage (baseline, 20% and 50% MVC, and recovery). Hence brachial artery blood flow was also estimated as stage-wise average, not in real time.

#### 2.4.2 DCS

The intensity autocorrelation function measured with the DCS system was analyzed to quantify the relative changes in muscle blood flow. Specially, the analytical solution of the correlation diffusion equation from a point source in a semi-infinite medium is given as:

$$G_1(r,\tau)=\frac{3\mu_s'}{4\pi}\left[\frac{e^{-K_D(\tau)r_1}}{r_1}-\frac{e^{-K_D(\tau)r_2}}{r_2}\right] \tag{1}$$

where $K_D(\tau)=\sqrt{3\mu_a\mu_s'+\mu_s'^2k_0^2\alpha\Delta r^2(\tau)}$ , $\mu_a$ is the absorption coefficient, $\mu_s'$ is the reduced scattering coefficient, $\alpha$ is the fraction of photon scattering events in the medium; $r_1=\sqrt{r^2+z_0^2}$ , $r_2=\sqrt{r^2+(z_0+2z_b)^2}$ , $r$ is the source–detector separation, $z_0=\frac{1}{\mu_s'}$ and $z_b=\frac{2(1+R_{eff})}{3(1-R_{eff})}$ , where $R_{eff}$ represents the effective reflection coefficient. $\langle\Delta r^2(\tau)\rangle$ represents the mean square displacement of the moving scatterers after a delay time $\tau$. The solution of $\langle\Delta r^2(\tau)\rangle$ can be derived from either the Brownian motion model or the random flow model. In this study we chose the Brownian motion model because it has been shown to fit the real correlation decay curves better over a wide range of tissue types [17]. In the case of Brownian motion $\langle\Delta r^2(\tau)\rangle=6D_B$ , where $D_B$ is the effective diffusion coefficient of the scatterers.

To fit the analytical solution into the measured intensity autocorrelation function, the analytical solution needs to be normalized to get $g_2(\tau)$ function:

$$g_2(\tau)=1+\beta\frac{|G_1(\bar{r},\tau)|^2}{\langle I(\bar{r},t)\rangle^2} \tag{2}$$

Biomedical Optics EXPRESS

where $I(\bar{r},t)$ is the detected diffusing light intensity at position $r$ and time $t$, and $\beta$ is a numerical factor related to the detector geometry, number of detected speckles and other experimental parameters. In this study a fixed value of $\beta = 1$ was used.

By minimizing the difference between the analytical solution and measured data of $g_2(\tau)$, we can yield a blood flow index given as BFI = $\alpha D_B$, where $\alpha$ represents the volume fraction of moving scatterers out of whole scatterers. Then, relative muscle blood flow from the initial baseline at $t_0$, rMBF, can be calculated as:

$$\text{rMBF} = \frac{\text{BFI}(t)}{\text{BFI}(t_0)} 100\%. \tag{3}$$

The absorption coefficient ($\mu_a$) and reduced scattering coefficient ($\mu_s'$) are required inputs in the fitting. In this study, each subject's $\mu_a$ and $\mu_s'$ values were measured prior to the experiment with a frequency-domain near-infrared tissue oximeter (OxiplexTS, ISS Inc., Champaign, IL) and then kept constant.

Further, the absolute light intensity measured with the DCS system over time, I($t$), was also analyzed to derive the changes in optical density, ΔOD, which is given as:

$$\text{OD} = log_{10}[\frac{\text{I}(t)}{\text{I}(t_0)}]. \tag{4}$$

The wavelength used in this study was 785 nm, which was very close to the isosbestic point of oxygenated hemoglobin ($HbO_2$) and deoxygenated hemoglobin (Hb) [18]. Therefore ΔOD primarily reflects absorption changes of total hemoglobin (HbT = $HbO_2$ + Hb).

## 3. Results

Fourteen subjects volunteered to participate. Five were not included in data analysis due to poor quality of Doppler ultrasound data ($n$ = 4) or DCS data ($n$ = 1). The results are reported on the remaining nine subjects (all males; age = 27.4 ± 2.9 years; BMI = 27.2 ± 3.8).

Figure 3 shows raw data of handgrip force, arterial blood pressure and brachial artery blood flow velocity from one representative subject. The subject was able to maintain relatively constant gripping force during both 20%-MVC and 50%-MVC exercise. Blood pressure increased gradually in these two stages. Brachial artery blood flow velocity increased moderately during 20%-MVC handgrip and exhibited large increase during 50%-MVC handgrip. As expected, reversal blood flow was observed during each contraction period, increasing with increased grip force [19–21].

Biomedical Optics EXPRESS

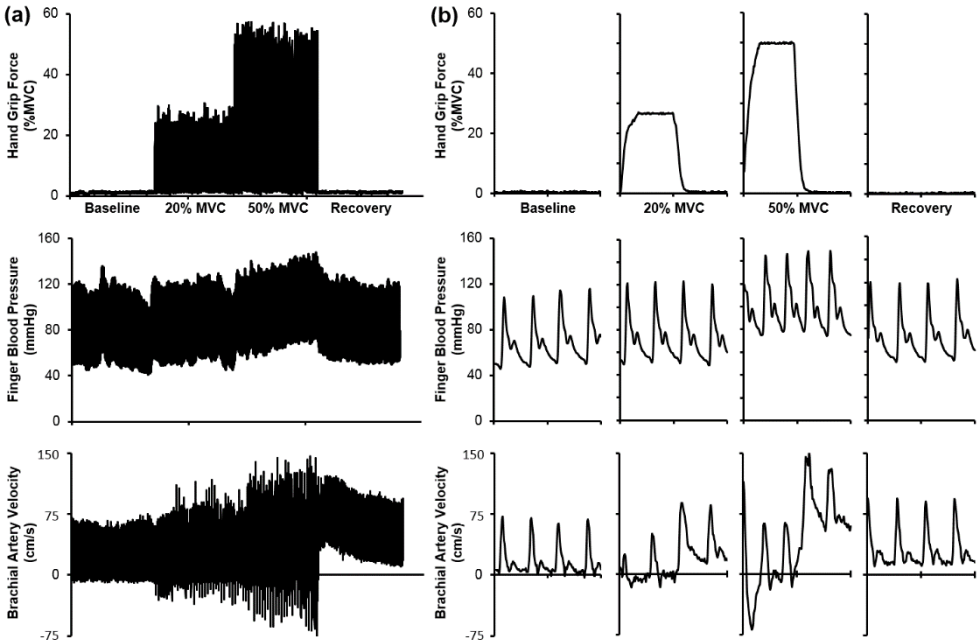


Fig. 3. Raw data of handgrip force (top), arterial blood pressure (middle) and brachial artery blood flow velocity (bottom) from one subject: (a) Real-time data throughout baseline, handgrip exercise at 20% and then 50% of maximal voluntary contraction (MVC), and post-exercise recovery. (b) Enlarged 4-second data segments in each stage: baseline, 20%-MVC and 50%-MVC handgrip exercise, and recovery.

### 3.1 Changes in arterial blood pressure

Figure 4 shows changes in mean arterial pressure at the group level. Significant changes were seen in each stage, i.e., an increase from baseline to 20%-MVC handgrip then to 50%-MVC handgrip, followed by a decrease during post-exercise recovery.

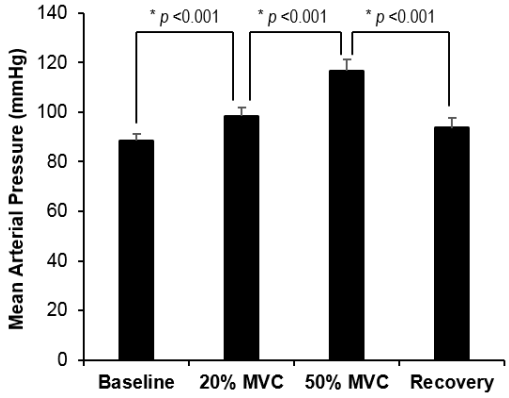


Fig. 4. Changes in mean arterial pressure (mean ± SE, $n$ = 9) through the four experimental stages: baseline, handgrip exercise at 20% and then 50% of maximal voluntary contraction (MVC), and post-exercise recovery. Differences between every two successive states were examined with paired $t$-test, and the $p$-values were corrected with the Bonferroni method for multiple comparisons.

### 3.2 Changes in blood flow

Brachial artery diameter measured with B-mode ultrasound did not change from baseline (0.35 ± 0.01 cm) to 20%-MVC handgrip (0.36 ± 0.01 cm), but increased significantly ($p$ <

Biomedical Optics EXPRESS

0.001, paired *t*-test) during 50%-MVC handgrip (0.38 ± 0.01 cm). This increase persisted into recovery stage (0.39 ± 0.01 cm).

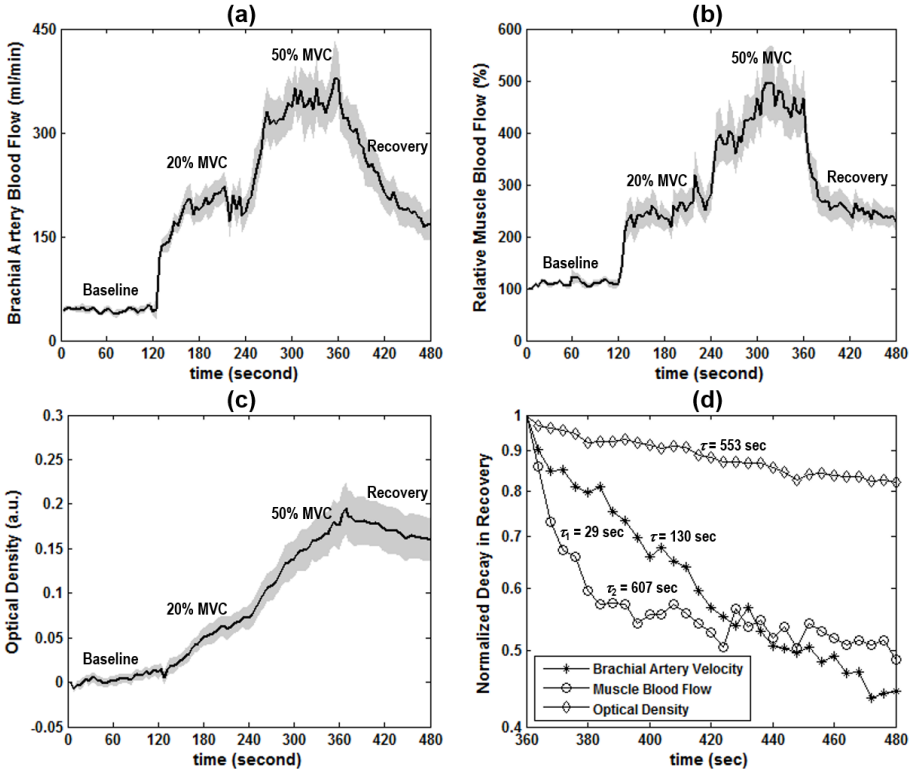


Fig. 5. Doppler ultrasound and DCS results at the group level: (a) to (c) Brachial artery blood flow velocity measured with Doppler ultrasound, regional muscle blood flow and optical density measured with DCS (mean ± SE, $n$ = 9). (d) Normalized decay of brachial artery blood flow velocity, regional muscle blood flow and optical density in recovery stage.

Figures 5(a) to 5(c) show changes in brachial artery blood flow velocity measured with Doppler ultrasound, local muscle blood flow and optical density measured with DCS at the group level. As illustrated, brachial artery blood flow velocity and local muscle blood flow had steady changes from baseline to 20%-MVC handgrip and then to 50%-MVC handgrip. These two readings had an excellent temporal agreement with each other ($R$ = 0.91 to 0.98 individually). In contrast, changes in optical density were slow and did not reach a plateau in any stage.

The main difference between Doppler ultrasound and DCS-derived readings was in the recovery from exercise. Figure 5(d) shows a close comparison among the normalized decay curves of brachial artery blood flow velocity, local muscle blood flow and optical density in the recovery stage: brachial artery blood flow velocity measured with Doppler ultrasound had a gradual decay throughout the recovery stage that was well fitted with an exponential process (time constant $\tau$ = 130 seconds) [22]. However, local muscle blood flow measured with DCS exhibited a biphasic feature: a sharp decay in the first phase ($\tau_1$ = 29 seconds) followed by a much slower decay in the second phase ($\tau_2$ = 607 seconds). The much slower decay in the second phase was very close to the gradual decay in optical density ($\tau$ = 553 seconds).

Biomedical Optics EXPRESS

### *3.3 Correlations of DCS-derived muscle blood flow with arterial blood pressure and Doppler ultrasound*

To better understand how global cardiovascular factors affected local muscle blood flow during exercise, and to evaluate the relationship between Doppler-derived and DCS-derived flow measures, linear correlation analyses were conducted. Because these changes were relatively stable during baseline, 20%-MVC and 50%-MVC handgrip exercise (not including recovery), 2-minute averaged data of each stage were used. Further, brachial artery blood flow velocity was integrated with brachial artery diameter (measured once in each stage with B-mode ultrasound imaging) to estimate the real brachial artery blood flow. As shown in Fig. 6, the brachial artery blood flow measured with Doppler ultrasound showed excellent correlation with DCS-derived muscle blood flow, as did mean arterial pressure.

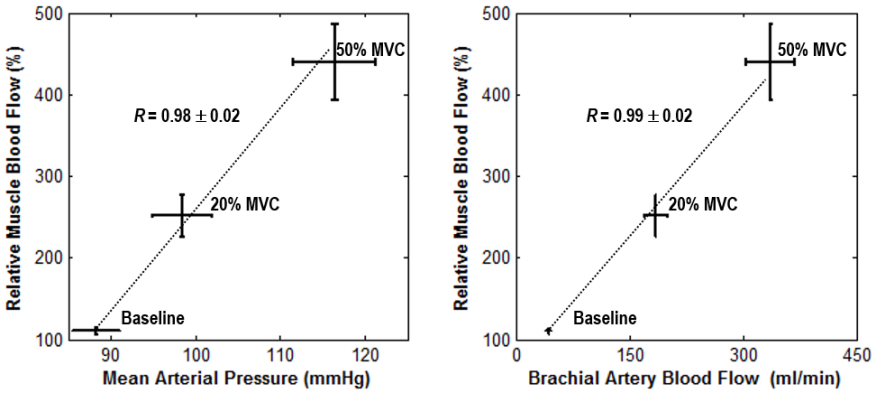


Fig. 6. Correlations of DCS-derived muscle blood flow with (a) mean arterial blood pressure and (d) brachial artery blood flow during baseline, 20%-MVC and then 50%-MVC handgrip exercise.

## 4. Discussion

To our knowledge, this is the first study to validate DCS-derived measurements of skeletal muscle blood flow during exercise. To accomplish our goal, we compared DCS with Doppler ultrasound, which is an established flow imaging modality commonly used to assess skeletal muscle blood flow during exercise. The major findings were two-fold: First, we demonstrate close agreement between DCS and Doppler ultrasound, both in terms of the magnitude of change and the temporal relationship. Second, we found that DCS was more reliable than traditional Doppler ultrasound, highlighting the clinical application of this new technology.

DCS is a relatively novel form of near-infrared technology to examine relative blood flow changes within deep tissues, especially for skeletal muscle (Table 1). While DCS has previously been validated against several different standards, as reviewed in the beginning of this paper, its validation in skeletal muscle during rhythmic exercise has not – to our knowledge – previously been performed. To address this limitation, we performed simultaneous recordings of skeletal muscle blood flow at rest and during rhythmic handgrip exercise using DCS and Doppler ultrasound. We chose Doppler ultrasound because it is by far the most widely used technique to assess skeletal muscle blood flow during exercise, providing strong external validity [12]. We show excellent agreement between these two modalities, supporting DCS is a valid measure of skeletal muscle blood flow.

Biomedical Optics EXPRESS

**Table 1. Summary of DCS studies on skeletal muscle blood flow**

| Reference | Sample size and study population | Muscle Studied and Protocol | Main Findings |
|---|---|---|---|
| Yu et al., 2005 [23] | 10 healthy, 1 patient with PAD | Gastrocnemius; 30 plantar flexion exercises (toe up-down) within one minute | In healthy subjects, plantar flexion increased relative blood flow 4.7 fold; 2.5-fold increase in the PAD patient. |
| Henry et al., 2015 [24] | 10 healthy | Gastrocnemius; 0.5Hz, 30% MVC | ~2.2 fold increase in relative blood flow |
| Gurley et al., 2012 [16] | 9 healthy | Forearm flexor muscle; handgrip exercise 25% MVC | ~5 fold increase in absolute blood flow |
| Shang et al., 2012 [25] | 14 women with fibromyalgia; 23 matched healthy controls | Vastus lateralus; 6 set of 12 isometric contractions of knee extensor exercise increasing from 20 to 70% MVC. Blood flow measured immediately post fatiguing exercise | ~200% increase in relative blood flow in patients and controls. |
| Present Data | 9 healthy men | Flexor digitorum profundus; 20% and 50% MVC handgrip exercise | 250% and 450% increase in relative blood flow with 20% and 50% HG, respectively |

Like other investigators before us [16, 26], our initial DCS experiments revealed significant motion artifact during muscle contraction (*data not shown*). To overcome this issue, some investigators have co-registered their dynamometer recordings and DCS measurements for offline correction of the blood flow data [26]. In contrast, we, and others [16], developed an online gating algorithm to synchronize data acquisition with the relaxation phase of each handgrip cycle. With this advancement, we were able to capture local muscle blood flow data in good quality at two distinct exercise intensities (20% and 50% MVC) in all subjects except one. In contrast, we were forced to exclude four of the original 14 subjects in this study due to data quality concerns with Doppler ultrasound, which is susceptible to motion artifact (particularly during higher intensity exercise). The DCS data quality was preserved in each of these cases, which highlights an important advantage of DCS over Doppler ultrasound. Indeed, the measurement of exercise skeletal muscle blood flow by Doppler ultrasound requires advanced training and practice for proficient and reliable data acquisition. DCS requires very little technical training, and is almost entirely operator independent.

While we observed good agreement between DCS and Doppler ultrasound during the plateau portion of each exercise intensity, we consistently observed transient differences in both the on-kinetics and off-kinetics for skeletal muscle blood flow between the two modalities. For example, during the recovery stage, note the gradual and consistent decay in Doppler ultrasound readings compared with the bi-phasic decay in DCS-derived muscle blood flow (Fig. 5(d)). These transient differences reflect key technical differences between the two modalities: while Doppler ultrasound measures the velocity of blood flow in a major artery based on the Doppler effect, DCS blood flow measurement is more complex. A recent study based on Monte Carlo simulations [27] showed that the DCS-derived blood flow index provides a direct measure of tissue blood flow, but is also sensitive to changes in hematocrit and average vessel diameter. For the DCS-derived muscle blood flow shown in Fig. 5(d), we interpret the first phase ($\tau_1$ = 29 seconds) as the blood flow changes in local microcirculation; whereas the second phase ($\tau_2$ = 607 seconds) reflects the heightened rate of oxygen delivery needed to support the increase in skeletal muscle oxygen demand post-exercise, which is slow to return to baseline. Indeed, the second phase has a very similar time constant to the gradual decay in optical density ($\tau$ = 553 seconds) that reflects absorption of total hemoglobin.

In conclusion, this study demonstrates an overall agreement and transient difference between DCS and Doppler ultrasound in measuring exercise skeletal muscle blood flow. Because skeletal muscle blood flow is a key determinant of aerobic capacity, which is an independent predictor of quality of life and cardiovascular disease morbidity and mortality,

Biomedical Optics EXPRESS

the finding from this study are highly relevant to the study of muscle physiology and pathology.

## Funding

Interdisciplinary Research Project of the University of Texas at Arlington; National Institutes of Health (NIH) (R03EB022956); American Heart Association (AHA) (15BGIA25860045).

## Disclosures

The authors declare that there are no conflicts of interest related to this article.